J Electroceram (2010) 24:219–225
DOI 10.1007/s10832-009-9561-3

Development of 2-2 piezoelectric ceramic/polymer composites by direct-write technique

J. Sun · P. Ngernchuklin · M. Vittadello · E. K. Akdoğan · A. Safari

Received: 11 April 2008 / Accepted: 8 January 2009 / Published online: 21 January 2009

Abstract The Micropen™ direct-write technique was used to fabricate ceramic skeletal structures to develop piezoelectric ceramic/polymer composites with 2–2 connectivity for medical imaging applications. A lead zirconate titanate PZT paste with ~35 vol.% solids loading was prepared as a writing material and the paste's rheological properties were characterized to evaluate its feasibly for Micropen deposition. A serpentine pattern was designed and deposited in AutoCAD and with a 100 μm pen tip, respectively. After debinding and sintering, the microstructural analysis showed that the ceramic structures were fully densified, with good bonding among layers. Typical single-layer thickness was ~50 μm, and sintered line width was ~120 μm. The composites containing 30–45 vol.% PZT were fabricated within 1 cm^2 area, with thicknesses ranging from 350 to 380 μm. Their electromechanical and dielectric properties were measured and found similar to that of composites fabricated by other techniques. The k_t was ~0.61, d_{33} was 210–320, with Q_m of ~6 and dielectric constant of 650–940.

J. Sun · P. Ngernchuklin · M. Vittadello · E. K. Akdoğan · A. Safari (✉)
The Glenn Howatt Electronic Ceramic Laboratory,
Department of Materials Science and Engineering,
Rutgers - The State University of New Jersey,
Piscataway, NJ 08854, USA
e-mail: safari@rci.rutgers.edu

J. Sun
e-mail: sunjj@eden.rutgers.edu

P. Ngernchuklin
e-mail: piyalak@eden.rutgers.edu

M. Vittadello
e-mail: vittadel@rci.rutgers.edu

E. K. Akdoğan
e-mail: eka@rci.rutgers.edu

Keywords Direct-write · Composites · Piezoelectric properties · PZT

1 Introduction

Lead zirconate titanate (PZT) is a widely used piezoelectric ceramic for transducer applications due to its excellent electromechanical properties, such as high dielectric constant (K), piezoelectric charge coefficient (d_{33}), and electromechanical coupling factor (k_t) [1]. PZT ceramic/polymer composites have drawn much attention because they combine the advantages of both ceramics and polymers, including high k_t, acoustic impedance close to that of issue, reasonably large dielectric constant and low mechanical loss. In particular, fine-scale PZT/polymer composites of different connectivities have been designed and investigated for ultrasonic medical imaging transducers operating at higher frequencies (1–30 MHz) [2–4].

Currently, PZT/polymer composites are commercially fabricated by injection molding, dice and fill and lost mold techniques. Other possible manufacturing methods include tape casting [5], micro-processing [6], laser cutting [7] and thermoplastic green machining [8]. However, these techniques are not suitable for building novel and complex designs within a short period of time. Because of the flexibility of direct-writing for miniaturization of composites, as well as the advantage of eliminating many processing steps such as cutting and mold-making, fabrication of composites by direct-write techniques has received increasing attention in recent years. Extensive research has been devoted to fused deposition of ceramics (FDC) [9, 10], robocasting [11, 12], stereolithography [13] and ink-jet printing [14]. These techniques allow depositing materials only where needed and enable rapid-prototyping

of novel or complex patterns for cost-effective small-lot production [15].

Another promising direct-write approach is Micropen™ system (Ohmcraft, Honeoye Falls, NY). It is a computer-automated device for precision printing of fluid slurries or pastes. The printed feature size is determined, although not exclusively, by pen tip sizes (inner diameter from 50 to 2,500 μm). A unique "dynamic pen control" feature enables writing on cambered or uneven substrates [16]. The Micropen direct-write provides the ability to fabricate multifunctional, multimaterial integrated ceramic components in an agile and rapid way. The original work on Micropen started in Sandia National Laboratories around 1997. Using commercially available screen printing thick-film slurries, Dimos and King et al. investigated the effects of paste rheology on print resolution and topography, and fabricated integrated, multilayer ceramic components (e.g. filter, inductors and voltage transformers) [17, 18]. Later, rheologically tailored, cofireable thick-film pastes for capacitor and varistor applications (e.g. lead zirconate niobium titanate and zinc oxide) were developed in Lewis' group [19, 20]. Previous work in our group was focused on direct-write of PZT and barium strontium titanate (BST) thick films for ferroelectric and capacitor applications [21–23].

Although Micropen™ direct-write has proven to be well suited for the deposition of thick films and multilayer devices, its capability of creating micro-scale three-dimensional (3D) structures has not been reported. The objective of our work is to utilize the Micropen technique to fabricate piezoelectric composites (300–400 μm in thickness) for transducers including medical imaging applications, bypassing the dicing or molding process. In what follows, the processing issues appertaining to Micropen™ direct write are discussed, and dielectric and piezoelectric properties of composites are provided.

2 Experimental

PZT pastes with 35, 40 and 45 vol.% solids loading were prepared for Micropen™ direct-write. Similar to our previous work [22], 5 vol.% ethyl cellulose was first dissolved in α-terpineol, to which a commercial PZT powder (TRS 610, TRS Ceramics) was gradually added into the terpineol-ethyl cellulose solution. The PZT powder was already coated with stearic acid in order to increase ceramic powder loading with having lower paste viscosity. After stirring for 20 min, the mixture was three-roll milled for 20 min to break agglomerates, by which paste uniformity was improved. Then, the paste was transferred into a syringe, and centrifuged to eliminate air bubbles generated during the preparation and handling. Finally, the syringe was loaded to Micropen for deposition.

A two-layer film was deposited as a bottom layer prior to depositing the PZT paste on an as-pressed PZT disc (as base), so as to promote co-densification during sintering. The PZT skeletal structure was deposited in a layer-by-layer build sequence to obtain the desired thickness. Underlying layers were dried under a lamp (15–30 min) before direct-writing on top of them. Two sizes of pen tips were used in our study (250 or 100 μm in inner diameter), for which Micropen direct-writing parameters (such as "cross section", "writing speed") were adjusted accordingly to achieve the required dimensions for the structures of interest.

The green PZT skeletal structures were debinded at 550°C with 1°C/min heating rate, followed by sintering at 1250°C for 1 h with 3.5°C/min heat rate in an excess-PbO atmosphere. The ceramic structures were then infiltrated with epoxy. The epoxy used was Epotek 301 (Epoxy Technology, MA, USA). Two different components of the epoxy were mixed in the weight proportion recommended by the manufacture. After magnetic stirring for 20 min, the epoxy was poured into a small plastic dish containing the sintered PZT structures. Vacuum deairing was performed by cycling between atmospheric pressure and ~−10 kPa several times until no bubbles generated from the samples. Then the samples were left in the vacuum chamber for 30 min under ~−10 kPa, followed by curing the epoxy at room temperature overnight. Upon curing the polymer, the infiltrated structures were polished to remove the PZT base. After electroding the composites by gold sputtering on both sides, poling was accomplished using 30 kV/cm for 15 min at 50°C.

The viscosities of the 35, 40 and 45 vol.% PZT pastes were measured with an AR1000-N rheometer (TA instrument) with a concentric cylinder, having conical end geometry. Line width and height of one-layer as-deposited PZT structure were measured with a profilometer (alpha-step 200, TENCOR Instruments). Thermogravimetric analysis (TGA) of the coated PZT powder and the 35 vol.% PZT paste was performed on Perkin-Elmer TGA7, in the range of 50–600°C at a heating rate of 10°C/min in air. The fracture surface of sintered structures was examined by field emission scanning electron microscopy (LEO-ZEISS, Gemini 982). Sintered density was evaluated by the Archimedes method.

The relative dielectric constant (K) and dielectric loss (tan δ) were determined with an impedance grain/phase analyzer (HP4194A, *Hewlett Packard)* at a frequency of 1 kHz at room temperature. The piezoelectric charge coefficient (d_{33}) was measured with a Berlincourt d_{33}-meter at 100 Hz (Model CPDT 3300, Channel Products, Chesterland, OH). The reported d_{33} values were an average of the composites since the probe covered the entire area of the samples. The electromechanical coupling factors (k_t, k_{31}) were determined by the resonance method [24], while the mechanical quality factor (Q_m) of the devices was evaluated by the bandpass method [25].

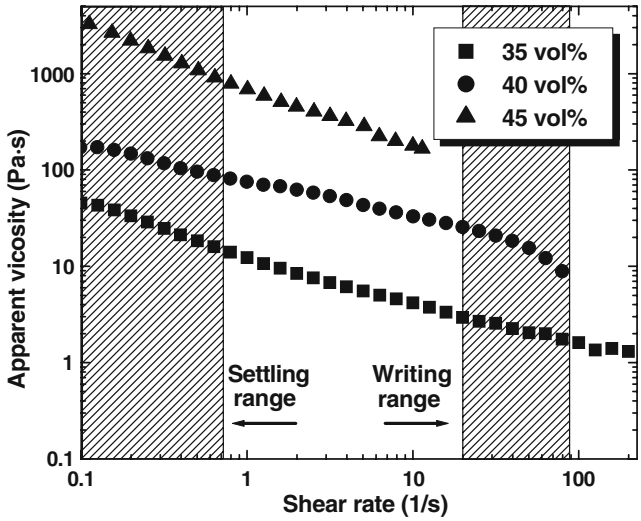

Fig. 1 Log–log plots of the apparent viscosity as a function of shear rate for the 35, 40 and 45 vol.% PZT pastes

3 Results and discussion

A key similarity with most direct-write techniques, which is also the case for Micropen deposition, is the importance of paste rheology. Figure 1 depicts the apparent viscosity as a function of shear rate for the 35, 40 and 45 vol.% PZT pastes. It is clear that all three pastes exhibited shear thinning behavior, and the viscosity increased as increasing solids loading in the shear rate range studied here. Shear thinning (or likewise shear thickening) behavior can be described by an empirical power law equation as [26]:

$$\eta_a = K\,\dot{\gamma}^{m-1} \tag{1}$$

where η_a is the apparent viscosity, $\dot{\gamma}$ is the shear rate, K is the consistency index, and m is the power-law index, which indicates the departure from Newtonian behavior. If $m<1$, Eq. 1 describes shear thinning. From Fig. 1, it is seen that K increased from 13.3 to 77.3 and to 741.3 with increasing solids loading, while m values were approximately 0.5, 0.4 and 0.6 for the 35, 40 and 45 vol.% pastes, respectively. The closeness of m values indicate that the degree of shear thinning for the three pastes were similar. As proposed by Dimos et al., the typical Micropen *writing range* corresponds to high shear rates (20–85 s^{-1}), while the material *settling range* corresponds to low shear rates (<1 s^{-1}) [17]. For the 35 vol.% PZT paste used in our Micropen deposition, the viscosities were 45 and 2 Pa·s in the *settling range* (0.1 s^{-1}) and *writing range* (85 s^{-1}), respectively. The relative high viscosity values in the *settling range* indicate that this paste can be used for writing high definition patterns. For the pastes with higher solids loading (e.g. 40 and 45 vol.%), problems due to possible agglomeration were encountered, although they exhibited higher viscosities. Therefore, the 35 vol.% paste was used in our current work, and the deposition using higher solids loading pastes was deferred to a future study.

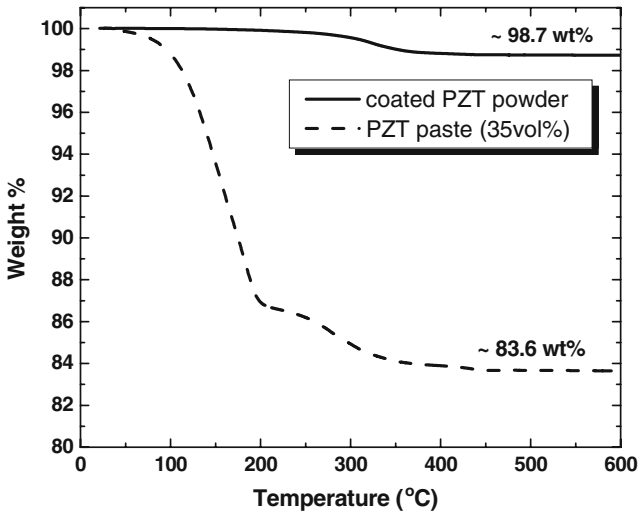

Fig. 2 TGA curves of the coated PZT paste and the 35 vol.% PZT paste

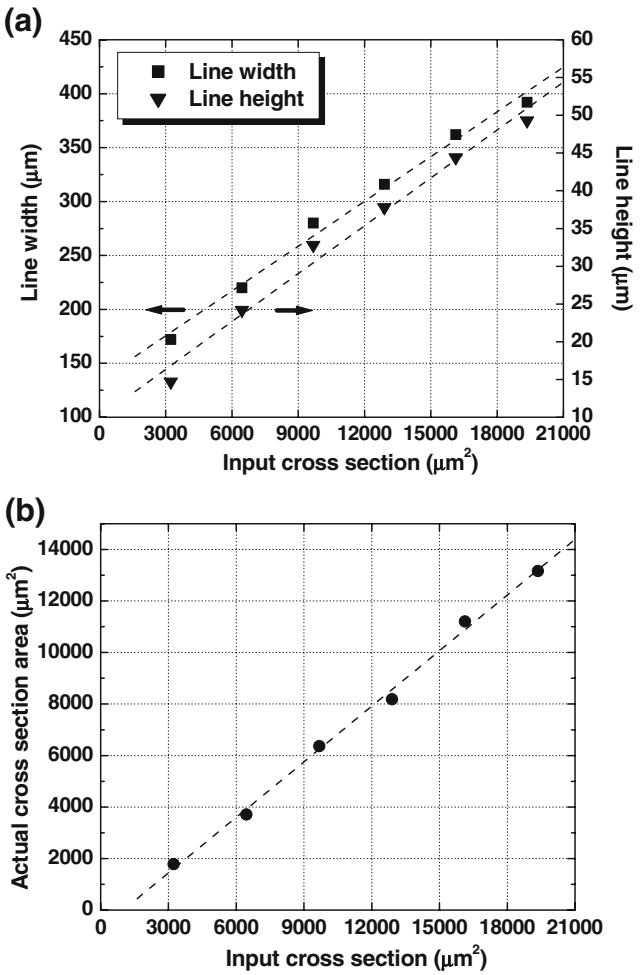

Fig. 3 The variations of (**a**) line width, line height and (**b**) actual cross section as a function of "input cross section (CS)"

TGA curves of the coated PZT powder and the 35 vol.% paste are plotted in Fig. 2. For the coated powder, it is found that approximately 1.3 wt.% stearic acid (as a dispersant) was absorbed onto the powder surface, which helped to avoid agglomerates. For the paste, the 84 wt.% residue at 600°C agreed with the calculated value (~81 wt.%) for the designed 35 vol.% paste. In addition, the weight losses below 200°C (~13 wt.%) and between 200–400°C (~3 wt.%) should be attributed to the solvent removal and the decomposition of the dispersant and binder, respectively.

To achieve uniform and consistent writing quality, various Micropen writing parameters should be optimized. For example, "cross section" (CS) of a printed line is one of the important parameters. It determines the amount of material delivered by a pen tip at a given writing speed, or can be simply defined as CS=line width (LW)×line height (LH) for an ideally rectangular cross-sectional line. Figure 3 plots the variations of LW, LH and actual cross section (ACS) as a function of "input CS". The test samples were one-layer deposition on glass slides, using a 100-μm diameter pen tip. The actual cross section (ACS) was automatically calculated from the deposited lines by a profilometer. Figure 3 illustrates LH, LW and ACS increased with increasing "input CS". And the relationship can be expressed using a linear fit equation of $y=A+Bx$ (shown in Fig. 2). Here, A and B give the slope and

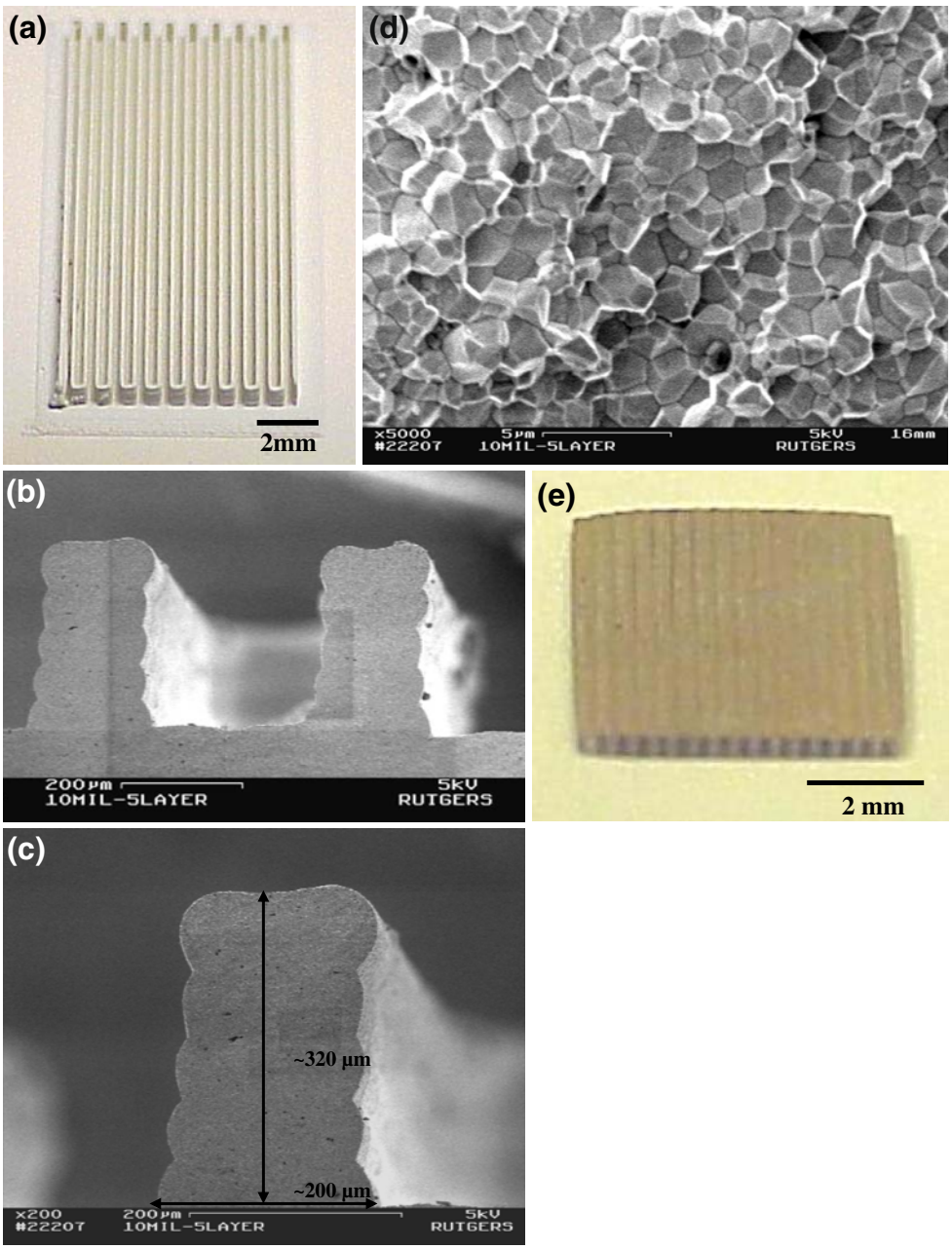

Fig. 4 (**a**) Image of the as-deposited ceramic structure for a composite A; (**b**), (**c**) and (**d**) FESEM micrograph of fracture surface of a sintered PZT plate; (**e**) image of the composite A after polymer infiltration, polishing and electroding

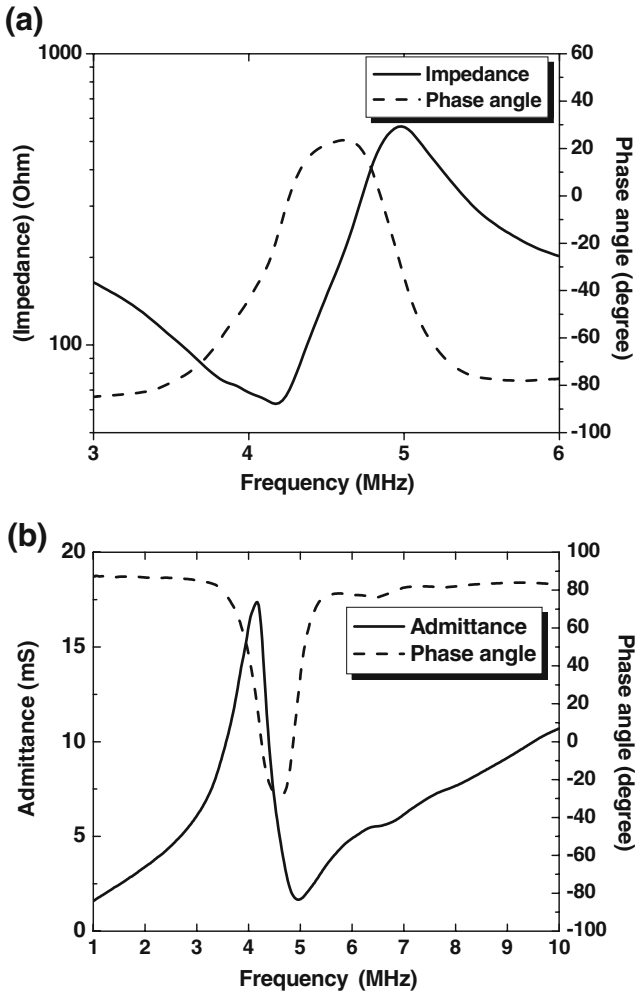

Fig. 5 (**a**) Impedance and phase angle spectra and (**b**) admittance and phase angle spectra of the composite A

intercept values, respectively, and *R* (correlation coefficient) representing the degree of linearity (the more *R* is closer to "1", the more the linearity). In detail, for the plot of LW, the values for *A*, *B* and *R* were 134.13, 0.014 and 0.99527, respectively; whereas for the plot of LH, *A*, *B* and *R* were 10.00, 0.0021 and 0.99194, respectively; While for the plot of ACS, *A*, *B* and *R* were −716.47, 0.72 and 0.99818, respectively. The nearly linear relation has been observed previously for thick films deposited by the Micropen, namely the film thickness linearly increased with CS [17, 21]. These results show that CS is a crucial parameter for controlling line dimensions. In addition, LH increased at the expense of increasing LW, which indicates that an optimal cross section should be chosen for a desired aspect ratio of PZT skeletal structures.

Figure 4(a) shows an as-deposited PZT skeletal structure for a 2–2 composite (composite A, deposited using a 100-μm pen tip). Although the Micropen deposition exhibits relatively good consistency and uniformity during writing in the "*stationary*" region, it is challenging to obtain high quality line starts and ends in the "*transient*" region. Therefore, a serpentine pattern was designed instead of separated lines. The same issue has been addressed in FDC and robocasting techniques [9, 12]. In addition, the sintering shrinkage of the ceramic plate width (~17%) was found to be similar to that of plate height (~19%). The similar tendency was also observed for the composites fabricated by thermoplastic green machining and FDC [8, 9]. Such shrinkage needs to be incorporated into the AutoCAD design in order to obtain required composite dimensions. Figure 4(b), (c) and (d) show the FESEM micrographs of sintered five-layer PZT plates (deposited using a 250-μm pen tip). First, FESEM reveals the typical cross section of ceramic structures in Micropen deposition. Similar to all solid freeform fabrication techniques, such feature originates from the layer-by-layer direct writing of cylindrical filament-based materials [9, 11, 12]. Secondly, multilayers were found to be bonded well and no delamination among layers after sintering. And the deposited layers were attached well on the substrate. Thirdly, a fully densified ceramic microstructure was obtained with grain size of 2–3 μm. Finally, for this sample, ~7% variation in line width and ~6% variation in line height were observed. Here, the typical single-layer thickness was ~60 μm, and the average maximum line width was ~200 μm. In general, deposited line dimensions are determined by a specific pen tip, paste material and writing parameters. The final composite A after polymer infiltration, polishing and electroding is shown in Fig. 4(e). After adjusting Micropen writing parameters, ~120 μm in line width and ~50 μm in line height were achieved for the typical one-layer sintered PZT structure using a 100-μm pen tip. The advantages of using a smaller pen tip are obtaining a higher aspect ratio (line height/line width) and finer scale, which is desirable to avoid lateral resonant waves and to increase d_{33} [8, 9]. However, dimension variations of ceramic plates and misalignment between layers may

Table 1 Comparison of dielectric and piezoelectric properties of a PZT disc and the two composites fabricated by Micropen.

Sample	PZT (vol.%)	Thickness (mm)	*K*	tan δ (%)	d_{33} (pC/N)	k_t	k_{31}	Q_m	Density (g/cm^3)
Bulk	100	0.93	2880	1.8	630	0.56	−0.38	20	7.77
Composite A	30	0.38	650	2.1	210	0.60	−0.36	7	3.18
Composite B	45	0.35	940	2.4	320	0.62	−0.34	6	4.20

become problems when using smaller pen tips mainly due to "agglomerates", which could be improved by optimizing paste processing [9].

Impedance and admittance spectra of the fundamental thickness mode resonance for the composite A are shown in Fig. 5. In this figure, sample A had a clean thickness mode resonance, with a resonant frequency of 4.1 MHz and an anti-resonant frequency of 5.0 MHz. Thus the thickness mode coupling coefficient (k_t) of ~0.60 was calculated according to the IEEE standard (listed in Table 1) [24]. In Fig. 5(b), the mechanical quality factor (Q_m) of ~7 was calculated.

Table 1 summarized the dielectric and piezoelectric properties of the two representative composites A and B (deposited using a 100-μm pen tip), along with a PZT bulk sample for comparison. The 31 mode coupling factors (k_{31}) of the composites were calculated from the resonance and anti-resonance frequencies of the lowest frequency resonance mode [24]. The planar mode coupling factors (k_p) of the composites could not be measured due to the rectangular geometry. The ceramic fractions were ~30 vol.% for composite A and ~45 vol.% for composite B. The ceramic volume fraction plays an important role in determining optimum efficiency both in transmitter and receiver modes for ultrasound transducers [27]. An attractive advantage of the Micropen direct-write is the design flexibility using AutoCAD software, thus desired volume fractions can be easily fabricated. The composite A had a k_t of 0.60 and Q_m of 7, while the values for the composite B were 0.62 and 6, respectively, which are comparable to what reported in literature using other techniques [5, 8, 9]. Compared to the bulk sample, the enhancement of k_t for the composites should be mainly caused by the partial relief of the lateral clamping in the polymer environment [28]. And the lower Q_m values obtained suggest that such composites are suited for the broad bandwidth applications, which is due to the partial damping of the ceramic plate's vibration by the surrounding polymer [29]. Table 1 also shows that the dielectric constant (K) of the composites was proportional to the ceramic volume fraction, as expected, because K does not depend on coupling between ceramic and polymer phases [30]. Furthermore, the d_{33} values were found to be 210 and 320 pC/N for the two volume fractions, indicating an increase with increasing ceramic volume fraction in our study. Different trends in the d_{33} variation with ceramic volume fraction have been observed [7, 12]. Because the d_{33} of composites is also affected by other factors such as the thickness of composites, the aspect ratio of the ceramic and the bonding between the ceramic and polymer phases, which all affect the stress transfer between the two phases [29, 31]. For the composites A and B, the thickness were about 380 and 350 μm, and the separation between the ceramic plates were about 260 and 170 μm, respectively.

4 Conclusions

PZT ceramic/polymer composites with 2–2 connectivity have been fabricated using Micropen™ direct-write technique. A 35 vol.% PZT paste was prepared for the Micropen deposition, which exhibited shear thinning behavior with a viscosity of ~45 Pa·s at lower shear rates (0.1 S^{-1}). It is found that "cross section", the Micropen writing parameter, is crucial for the dimensional control in deposition.

The deposited ceramic skeletal structures were fully densified, with good bonding among layers. The composites (thickness=350–380 μm) had resonance frequencies at ~4 MHz, and satisfactory electromechanical properties (k_t= 60–62%, Q_m=6–7, d_{33}=210–320, K=650–940 and tan δ= 2.1–2.4%). Such results indicate that the Micropen direct-write has the potential to fabricate miniaturized 2–2 composites and other novel composites for medical imaging applications.

Acknowledgements The authors gratefully acknowledge the financial support of the Glenn Howatt Foundation at Rutgers University.

References

1. B. Jaffe, W.R. Cook, H. Jaffe, *Piezoelectric Ceramics*. (Academic, New York, 1971), pp. 271–280
2. T.R. Gururaja, A. Safari, N.E. Newnham, L.E. Cross, in *Electronic Ceramics*, ed. by L.M. Levinson (Marcel Dekker, New York, 1987), pp. 93–145
3. A. Safari, M. Allahverdi, E.K. Akdogan, J. Mater. Sci. **41**, 177 (2006). doi:10.1007/s10853-005-6062-x
4. V.F. Janas, A. Safari, J. Am. Ceram. Soc. **78**(11), 2945 (1995). doi:10.1111/j.1151-2916.1995.tb09068.x
5. W. Hackenberger, S. Kown, P. Rehrig, in *Proc. of the IEEE Ultrason. Symp*. 1253 (2002)
6. J. Park, S. Lee, S. Park, J. Cho, S. Jung, J. Han, S. Kang, Sens. Actuators A Phys. **108**, 206 (2003). doi:10.1016/S0924-4247(03)00362-5
7. K. Li, D.W. Zeng, K.C. Yung, H.L.W. Chan, C.L. Choy, Mater. Chem. Phys. **75**, 147 (2000). doi:10.1016/S0254-0584(02)00044-5
8. Y.H. Koh, C.B. Yoon, S.M. Lee, H.E. Kim, J. Am. Ceram. Soc. **88**(4), 1060 (2005). doi:10.1111/j.1551-2916.2005.00210.x
9. G.M. Lous, I.A. Cornejo, T.F. McNulty, A. Safari, S.C. Danforth, J. Am. Ceram. Soc. **83**(1), 12 (2000). doi:10.1111/j.1151-2916.2000.tb01159.x
10. S. Turcu, B. Jadidian, S.C. Danforth, A. Safari, J. Electroceram. **9**, 165 (2002). doi:10.1023/A:1023209107995
11. J.A. Lewis, J. Am. Ceram. Soc. **89**(12), 3599 (2006). doi:10.1111/j.1551-2916.2006.01382.x
12. J.E. Smay, J. Cesarano III, B.A. Tuttle, J.A. Lewis, J. Am. Ceram. Soc. **87**(2), 293 (2004). doi:10.1111/j.1551-2916.2004.00293.x
13. O. Dufaud, P. Marchal, S. Corbel, J. Eur. Ceram. Soc. **22**, 2081 (2002). doi:10.1016/S0955-2219(02)00036-5
14. R. Noguera, M. Lejeune, T. Chartier, J. Eur. Ceram. Soc. **25**, 2055 (2005). doi:10.1016/j.jeurceramsoc.2005.03.223

15. A. Piqué, D.B. Chrisey, in *Direct-Write Technologies for Rapid Prototyping Applications: Sensors, Electronics, and Integrated Powder Sources*, ed. by A. Piqué, D.B. Chrisey (Academic, New York, 2001), pp. 1–11
16. P.G. Clem, N.S. Bell, G.L. Brennecka, B.H. King, D.B. Dimos, in *Direct-Write Technologies for Rapid Prototyping Applications: Sensors, Electronics, and Integrated Powder Sources*, ed. by A. Piqué, D.B. Chrisey (Academic, New York, 2001), pp. 229–256
17. D. Dimos, P. Yang, T.J. Garino, M.V. Raymoud, M.A. Rodriguez, in *Proc. of Solid Freeform Fabrication Symp*., Austin, TX, University of Texas at Austin, 133 (1999)
18. B.H. King, D. Dimos, P. Yang, S.L. Morissette, J. Electroceram. **3** (2), 173 (1999). doi:10.1023/A:1009999227894
19. S.L. Morissette, J.A. Lewis, P.G. Clem, J. Cesarano III, D.B. Dimos, J. Am. Ceram. Soc. **84**(11), 2462 (2001)
20. V. Tohver, S.L. Morissette, J.A. Lewis, B.A. Tuttle, J.A. Voigt, D. B. Dimos, J. Am. Ceram. Soc. **85**(1), 123 (2002)
21. J. Sun, M. Vittadello, E.K. Akdogan, A. Safari, in *Proc. of the 15th IEEE International Symposium on the Applications of Ferroelectrics (ISAF)* 57 (2006)
22. M. Allahverdi, A. Safari, in *Proc. of the 14th IEEE International Symposium on the Applications of Ferroelectrics (ISAF)*, 250 (2004)
23. M. Kunduraci, W.K. Simon, E.K. Akdogan, A. Safari, in *Proc. of the 14th IEEE International Symposium on the Applications of Ferroelectrics (ISAF)*, 21 (2004)
24. IEEE, Standard on Piezoelectricity, ANSI/IEEE Std. 176, (the Institute of Electrical and Electronics Engineers (IEEE), Inc., New York, 1987)
25. E.K. Akdoğan, M.S. Thesis, METU, Ankara, Turkey (1994)
26. J.S. Reed, *Principles of Ceramics Processing*, 2nd edn. (Wiley, New York, 1995)
27. D.D.N. Hall, J.T. Bennett, G. Hayward, in *Proc. of Soc. Photo-Opt. Instrum. Eng.(SPIE)* **1733**, 216 (1992)
28. W.A. Smith, in *Proc. of IEEE Ultrason. Symp*. Montreal, Canada, **2**, 755 (1989)
29. T.R. Gururaja, W.A. Schulze, L.E. Cross, IEEE Trans. Sonics Ultrason. **SU-32**, 481 (1985)
30. T.R. Gururaja, R.E. Newnham, K.A. Klicker, in *Proc. of Ultrason. Symp.* 576 (1980)
31. W. Cao, Q.M. Zhang, L.E. Cross, IEEE Trans. on Ultrason. Ferroelec. Freq. Contr. **40**(2), 103 (1993). doi:10.1109/58.212557